Direct Imaging of Exoplanets: Science & Techniques
Proceedings IAU Colloquium No. 200, 2005
C. Aime and F. Vakili, eds.

doi:10.1017/S1743921306009999

Speckle statistics in direct and coronagraphic imaging

Rémi Soummer[1]†, Claude Aime[2], André Ferrari[2], Anand Sivaramakrishnan[1], Laurent Jolissaint[3], James Lloyd[4], Ben R. Oppenheimer[1], Russell Makidon[5], and Marcel Carbillet[2]

[1]American Museum of Natural History, 79th St at Central Park West, New York, USA
email: rsoummer@amnh.org, anand@amnh.org, bro@amnh.org

[2]Laboratoire Universitaire d'Astrophysique de Nice, Parc Valrose, Nice, France
email: Claude.Aime@unice.fr, Andre.Ferrari@unice.fr

[3]Herzberg Institute of Astrophysics, 5071 West Saanich Road, Victoria, B.C. V9E 2E7, Canada
email: laurent.jolissaint@nrc-cnrc.gc.ca

[4]Department of Astronomy, Cornell University, Ithaca, NY 14853, USA
email: jpl@astro.cornell.edu

[5]Space Telescope Science Institute, 3700 San Martin Drive, Baltimore, USA
email: makidon@stsci.edu

Abstract. In this communication, we study the statistical properties of the light intensity in direct and coronagraphic images, in the context of ground-based Extreme Adaptive Optics observations. The same approach can also be used for space observations with different scales. We show that a coronagraph only affects the perfect part of the wave and leaves the uncorrected part of the wavefront almost unaffected. This statistical model can explain the 'speckle pinning' effect (presence of speckles at the position of the diffraction rings), as an amplification of the speckle noise. This statistical approach can be verified on real adaptive optics data.

Keywords. instrumentation: high angular resolution, instrumentation: adaptive optics.

1. Introduction

Direct imaging of a faint companion around a bright star is a difficult task, where the contrast ratio and the angular separation are the relevant observable parameters. The problem consists of detecting a faint source on top of a bright background mainly caused by the star diffracted light. In the case of ground-based observations with adaptive optics, the residual uncorrected aberrations produce random intensity fluctuations of the background, and lead to the presence of speckles in the field. In direct non-coronagraphic images, these speckles mainly appear at the position of the diffraction rings of the star. This phenomenon, also known as 'speckle pinning', Bloemhof et al. (2001), can be explained using a statistical model showing that the speckle fluctuation is amplified at the position of the diffraction rings.

2. Statistical properties of residual speckles in AO- corrected coronagraphic images

In this section, we study the statistical properties of speckles after a coronagraph, for ground based observations using Extreme Adaptive Optics (ExAO). This presentation extends that of Aime & Soummer (2004a), and Aime & Soummer (2004b).

† Michelson Fellow

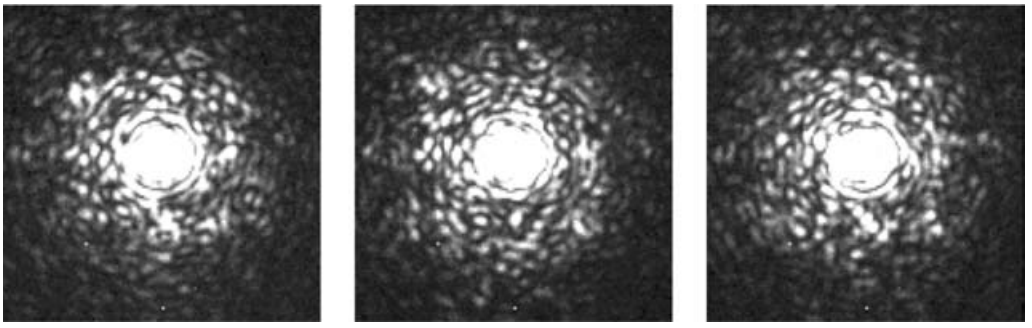

Figure 1. Direct (non-coronagraphic) PSFs from Palomar with AO. The narrow band, short exposures show that the speckles are preferentially located at the position of the PSF rings (speckle pinning). The fluctuations of these speckles is the main source of noise in high contrast imaging.

We consider an instrument with an ExAO system and a generic coronagraph to accomodate any type of focal plane mask designs. We denote by the subscripts 1,2,3,4 the four successive coronagraphic planes: the first plane corresponds to the entrance aperture (possibly apodized), the second plane is the focal plane where a coronagraphic mask is applied, the third plane corresponds to a relay pupil plane where a diaphragm is applied (the Lyot Stop), and finally the fourth plane corresponds to the final focal plane.

Following the notations of Aime & Soummer (2004a), at any instant, we can write the wavefront complex amplitude at the entrance pupil as the coherent sum of two terms, a deterministic term A corresponding to a perfect plane wave, and a random term $a(\mathbf{r})$ corresponding to the uncorrected part of the wavefront. This term $a(\mathbf{r})$ can also include either phase or amplitude errors and has zero mean:

$$\Psi_1(\mathbf{r}) = [A + a(\mathbf{r})]\ P(\mathbf{r}), \tag{2.1}$$

where the function $P(\mathbf{r})$ describes the aperture transmission, and $\mathbf{r} = (x, y)$ is the coordinate vector, used in both pupil and field.

In the first focal plane, a coronagraphic mask is applied at the center of the image of the star image. Writing the mask transmission as $1 - M(\mathbf{r})$, allows to accomodate any type of mask coronagraphs. For example, a classical hard-edged Lyot coronagraph, is described using a top-hat function for M. The complex amplitude of the wave in the focal plane is given by a scaled Fourier Transform (FT) of this pupil amplitude Goodman (1996):

$$\Psi_2(\mathbf{r}) = \frac{1}{\imath\lambda f}\ \mathcal{F}[\Psi_1(\mathbf{r})]\,(1 - M(\mathbf{r}))\,, \tag{2.2}$$

where the symbol $\widehat{\ }$ denotes the FT, f the telescope focal length, λ the monochromatic wavelength, and the notation $\mathcal{F}$ the scaled FT:

$$\mathcal{F}[\Psi_1(\mathbf{r})] = \widehat{\Psi}_1\left(\frac{\mathbf{r}}{\lambda f}\right). \tag{2.3}$$

For clarity, we will omit in the following the scaling factor $1/\imath\lambda f$ that appears between each of the planes, as a proper re-scaling leads to the same result, and we have:

$$\Psi_2(\mathbf{r}) = (A\,\mathcal{F}[P(\mathbf{r})] + \mathcal{F}[a(\mathbf{r})\,P(\mathbf{r})])\ \ (1 - M(\mathbf{r}))\,, \tag{2.4}$$

In the next pupil plane, the complex amplitude before the Lyot stop $P'(\mathbf{r})$ is:

https://doi.org/10.1017/S1743921306009999 Published online by Cambridge University Press

$$\Psi_3(\mathbf{r}) = A\,P(\mathbf{r}) - \frac{1}{\lambda^2 f^2}\,A\,P(\mathbf{r}) * \mathcal{F}[M(\mathbf{r})] + a(\mathbf{r})P(\mathbf{r}) - \frac{1}{\lambda^2 f^2}\,a(\mathbf{r})P(\mathbf{r}) * \mathcal{F}[M(\mathbf{r})] \tag{2.5}$$

The first line is proportional to the Lyot stop complex amplitude for a perfect coronagraph Soummer *et al.* (2003). The factor $1/\lambda^2 f^2$ is due to the two-dimension change of variable in the convolution product. In the case of an APLC, the Lyot stop is identical to the pupil. In either case, we have: $P(\mathbf{r})P'(\mathbf{r}) = P'(\mathbf{r})$.

In the final focal plane, with the notations $S(\mathbf{r}) = \mathcal{F}[a(\mathbf{r})\,P'(\mathbf{r})]$, we obtain:

$$\Psi_4(\mathbf{r}) = A\,\Psi_{coro}(\mathbf{r}) + S(\mathbf{r}) - \frac{1}{\lambda^2 f^2}(S(\mathbf{r})M(\mathbf{r})) * \mathcal{F}[P'(\mathbf{r})], \tag{2.6}$$

where Ψ_{coro} denotes the focal wave amplitude of the coronagraph in the perfect case.

The convolution term of Eq.2.6 can be neglected outside the mask area: the extension of the term $S(\mathbf{r})M(\mathbf{r})$ is limited to the mask size and the equivalent width of $\mathcal{F}[P'(\mathbf{r})]$ is one resolution element. Therefore, the spatial extension of their convolution product is limited approximately to the mask size, which is illustrated in Fig. 2.

Figure 2. illustration corresponding to Eq.2.6. Left is the speckle term $S(\mathbf{r}) = \mathcal{F}[a(\mathbf{r})\,P(\mathbf{r})]$ (modulus). Center: the cross term $S(\mathbf{r})M(\mathbf{r}) * \mathcal{F}[P'(\mathbf{r})]$. This illustrates that the cross-terms can be neglected outside the mask area. Right: Modulus of the subtraction of the two amplitudes: this shows there is no modification outside the central region corresponding to the mask size.

We obtain a similar expression to the case without coronagraph with $C(\mathbf{r}) = A\,\mathcal{F}[P(\mathbf{r})]$ Aime & Soummer (2004a):

$$\Psi_4(\mathbf{r}) = \tilde{C}(\mathbf{r}) + S(\mathbf{r}). \tag{2.7}$$

The wave amplitude after a coronagraph appears as a sum of a deterministic term $\tilde{C}(\mathbf{r})$, and a random term $S(\mathbf{r})$, at each position in the focal plane, outside the mask area. The term $\tilde{C}(\mathbf{r})$ corresponds to the focal amplitude after the coronagraph. Static aberrations (deterministic) can also be included in this term. The second component is a random term, associated with the speckles, identical to that of Aime & Soummer (2004a): $S(\mathbf{r}) = \mathcal{F}[a(\mathbf{r})\,P(\mathbf{r})]$. The coronagraph has a negligible effect of the speckle part, as illustrated and Fig. 2.

In the case of coronagraphic images as well as in direct images Aime & Soummer (2004a), the statistics of the focal plane complex amplitude follows a non-central gaussian statistics. This problem is formally equivalent to the study of laser speckles over a coherent background in the context of holography. The probability density function

https://doi.org/10.1017/S1743921306009999 Published online by Cambridge University Press

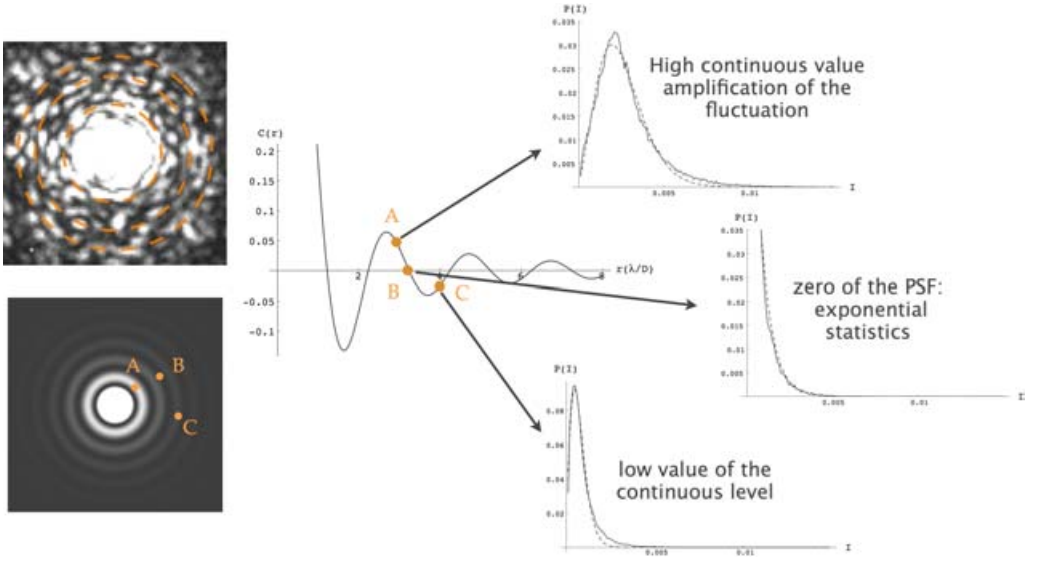

Figure 3. Probability Density Function of the light intensity at 3 different positions in the focal plane, corresponding to different background field amplitude C(r) (or intensity levels Ic. The hard lines correspond to the result of a numerical simulation using 3000 instantaneous PSF (PAOLA Software, Jolissaint 2004). The dotted curves correspond to the theoretical model fitted to the numerical simulations.. The width of the distribution clearly increases with an increase in the level of the constant intensity background: this explains speckle pinning: speckle fluctuations are amplified by the constant background corresponding to the perfect part of the wave.

(PDF) of $\Psi_2(x, y)$ was given by Goodman (1975):

$$\mathcal{P}(\xi, \eta) = \frac{1}{\pi < |S(x,y)|^2 >} \exp\left(\frac{-(\xi - C(x,y))^2 + \eta^2}{< |S(x,y)|^2 >}\right), \tag{2.8}$$

where ξ and η denote the real and imaginary part of $\Psi_2(x, y)$ at the position (x, y).

The corresponding PDF for the intensity, known as a *modified Rician density*, was given by Goodman (1975) and also used by Cagigal and Canales (1998), Cagigal and Canales (2000):

$$\mathcal{P}_I(I) = \frac{1}{I_s} \exp\left(-\frac{I + I_c}{I_s}\right) \mathrm{I}_0\left(\frac{2\sqrt{I}\sqrt{I_c}}{I_s}\right), \tag{2.9}$$

where I_0 denotes the zero-order modified Bessel function of the first kind. This PDF is also valid in the case of coronagraphic images, I_c being the coronagraphic response to a perfect wave. A numerical simulation is shown in Fig. 3 to illustrate this Rician distribution. The intensity statistics are generated from the simulated PSFs, at a given radius. PDFs examples are given for three different radii, one at the top of an Airy ring (strong pinning effect), one at a PSF zero (no speckle pinning) and one at an intermediate position.

Speckle pinning can be easily explained from the analysis of these intensity PDFs: speckle intensity and fluctuations are amplified by the coherent part of the wave amplitude $C(r)$, or intensity I_c. This can be seen directly on the PDFs in Fig. 3, where the widths increase with I_c. Depending on the amplitude of the Airy pattern at successive rings, the intensity I_c is alternatively large and small and the variance of the speckles is amplified accordingly. At the zeroes of the PSF, no amplification occurs and the statistics is equivalent to that of a fully developed speckle pattern (exponential statistics). In the

https://doi.org/10.1017/S1743921306009999 Published online by Cambridge University Press

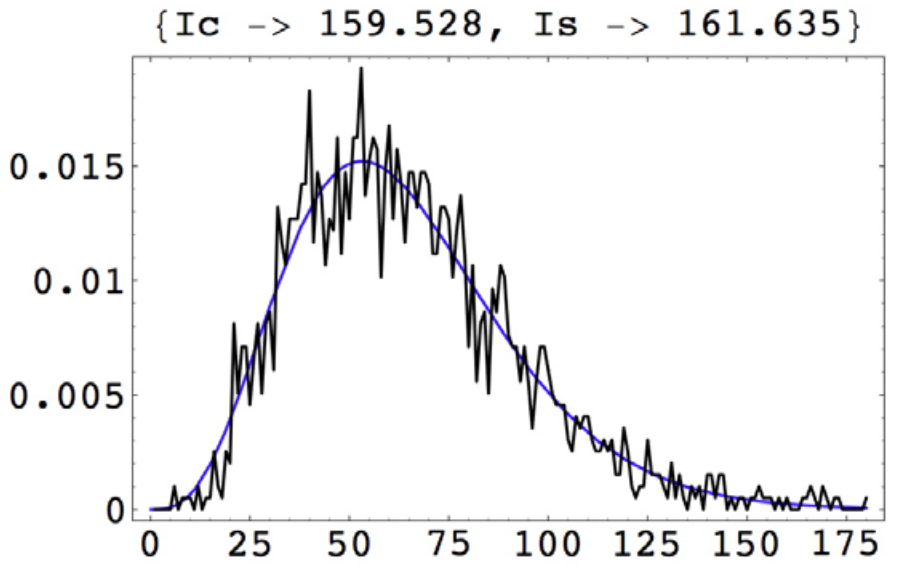

Figure 4. This is the comparison between the empirical PDF and the statistical model, for a given pixel in the field. The model used here corresponds to the integration of 4 independent speckle realizations. The empirical PDF at this location has been obtained using 1500 short exposure images in the K-band with the Palomar AO system.

case of a perfect coronagraph, speckle pinning is totally suppressed and all the residual speckles are similar to laser speckles with exponential statistics.

These statistics has been verified on direct images (non-coronagraphic) by Fitzgerald & Graham (2005) using AO data at the Lick Observatory. Using data from Palomar, we also find good agreement between the statistical model and the data. The data consists of non-coronagraphic images, obtained with the Palomar AO system and narrow band filters in the K-band. The exposure times of 120ms integrate several realizations of speckles, assuming a typical lifetime of 30-40 ms in K-band. It is possible to generalize the rician model to obtain the PDF for the sum of M independant speckle realizations. The corresponding statistics for such integrated speckles is also known as a non-central chi square distribution of order M:

$$\mathcal{P}(I) = \frac{M}{I_s}\left(\frac{I}{I_c}\right)^{\frac{M-1}{2}} e^{-\frac{M(I+I_c)}{I_s}} I_{M-1}\left(\frac{2\sqrt{I}\sqrt{I_c}M}{I_s}\right) \tag{2.10}$$

Using a Kolmogorov-Smirnov test, it is possible to study the compatibility between the model and the data as a function of the speckle lifetime. We find the best agreement between model and data for $M = 4$ (sum of 4 independent realizations in each exposure), which is compatible with the expected lifetime in K-band. We give an example in Fig. 4 where a good agreement is obtained between data and model.

A direct application of this statistical model is to provide the variance of the speckle noise which can be used for further simulations to predict the performance of instruments with coronagraphs.

Acknowledgements

Rémi Soummer is supported by a Michelson Fellowship, under contract with the Jet Propulsion Laboratory funded by NASA. JPL is managed for NASA by the California Institute of Technology.

https://doi.org/10.1017/S1743921306009999 Published online by Cambridge University Press

References

Aime, C. & Soummer, R., 2004, *ApJ*, 612, L85
Aime, C. & Soummer, R., 2004, *EAS Publications Series*, 12, 89
Aime, C., Soummer, R., & Ferrari, A., 2002, *A&A*, 389, 334
Bloemhof, E. E., Dekany, R. G., Troy, M., & Oppenheimer, B. R., 2001, *ApJ* 558, L71
Bloemhof, E. E., 2003, *ApJ* 582, L59
Cagigal, M. P. & Canales, V. F., 1998, *Optics Letters* 23, 1072
Cagigal, M. P. & Canales, V. F., 2000, *JOSA* 17, 1312
Fitzgerald, M. & Graham, J., 2005, *ApJ preprint doi:10.1086/'498339'*
Goodman, J., 1975, in *topics in applied physics: laser speckle and related phenomena, Dainty Ed.*, springer verlag berlin
Goodman, J., 1996, *Introduction to Fourier Optics*, Mac Graw Hill
Soummer, R., Aime, C., & Falloon, P. E., 2003, *A&A*, 397, 1161